Photoinduced Electron Transfer to C_{60} across Extended 3- and 11-Bond Hydrocarbon Bridges: Creation of a Long-Lived Charge-Separated State

René M. Williams,*,† Mattijs Koeberg,† James M. Lawson,‡ Yi-Zhong An,§ Yves Rubin,*,§ Michael N. Paddon-Row,*,‡ and Jan W. Verhoeven*,†

Laboratory of Organic Chemistry, University of Amsterdam, Nieuwe Achtergracht 129, 1018 WS Amsterdam, The Netherlands, School of Chemistry, University of New South Wales, Sydney, New South Wales 2052, Australia, and Department of Chemistry and Biochemistry, University of California, Los Angeles, California 90095-1569

Received April 12, 1996[⊗]

Two new, rigid donor−bridge−C_{60}(acceptor) dyads are presented. In one system (**C_{60}[3]TMPD**) a 3-σ-bond bridge separates the fullerene from a powerful tetraalkyl-*p*-phenylenediamine donor; in the other (**C_{60}[11]DMA**) the bridge comprises an extended array of 11 bonds, while the donor unit is a dimethylaniline group. Photoexcitation of the 3-bond system induces fast ($k_{cs} \geq 1.6 \times 10^{10}$ s^{-1}) and virtually complete intramolecular charge separation, irrespective of solvent polarity. It is concluded that this charge separation occurs under nearly "optimal" conditions. Charge recombination, however, is also very fast, preventing the detection of the charge-separated state on a nanosecond time scale. For the 11-bond system, photoinduced charge separation only occurs in polar solvents, reaching $k_{cs} = 5.5 \times 10^9$ s^{-1} in benzonitrile, which still implies a charge separation yield of ∼90%. Interestingly, charge recombination is now slowed down considerably, thereby allowing easy detection of the "giant dipolar" charge-separated state of **C_{60}[11]DMA** with a lifetime of *ca.* 0.25 μs. The experimental results, together with semiempirical MO calculations, indicate that the special symmetry properties of the fullerene π-system may cause it to enter into very strong electronic coupling with the hydrocarbon bridge to allow fast photoinduced charge separation, while at the same time the electronic coupling relevant for charge recombination remains small.

Introduction

Fullerenes[1,2] are characterized by remarkably strong electron-accepting properties.[3] Stable multianions can been generated,[4] in contrast to the corresponding cationic species, which are very unstable.[5] The electron-accepting properties of fullerenes, in combination with their electronic absorption characteristics[6] extending over most of the visible region, make them promising chromophores in photodriven redox processes. This has, for example, been demonstrated from the observation of intermolecular quenching of both the excited singlet and triplet state of fullerenes by various electron donor species[7] and by the observation of various photoreactions that can be formulated to emerge from primary electron transfer.[8]

The synthesis of several donor−bridge−fullerene(acceptor) systems has been reported,[9] but in only a few cases has intramolecular photoinduced charge separation been reported to occur.[7a,10] In these cases, which all involve a relatively short bridge, the rate of (thermal) charge recombination is very high, which typically brings the lifetime of the charge-separated state in the sub-nanosecond regime, thereby severely limiting its possibility to enter into further redox processes. In the case of the system **C_{60}[3]DMA** (see Figure 1), photoinduced charge separation and charge recombination both occur on a sub-nanosecond time scale (in benzonitrile).[7a]

Because charge separation in **C_{60}[3]DMA** is limited to polar solvents, we have investigated the **C_{60}[3]TMPD** system, in which the **DMA** chromophore (**DMA** = *N*,*N*-dimethylaniline) is replaced by the considerably stronger **TMPD** donor (**TMPD** = *N*,*N*,*N*′,*N*′-tetramethyl-*p*-phenylenediamine), in order to see whether it is possible to induce charge separation in nonpolar media. Furthermore, we have extended the length of the bridge from 3

† University of Amsterdam.
‡ University of New South Wales.
§ University of California.
⊗ Abstract published in *Advance ACS Abstracts,* July 1, 1996.

(1) Kroto, H. W.; Heath, J. R.; O'Brien, S. C.; Curl, R. F.; Smalley, R. E. *Nature* **1985**, *318*, 162.
(2) Krätschmer, W.; Lamb, L. D.; Fostiropoulos, K.; Huffman, D. R. *Nature* **1990**, *347*, 345.
(3) Allemand, P. M.; Koch, A.; Wudl, F.; Rubin, Y.; Diederich, F.; Alvarez, M. M.; Anz, S. J.; Whetten, R. L. *J. Am. Chem. Soc.* **1991**, *113*, 1050.
(4) Xie, Q.; Perez-Cordero, E.; Echegoyen, L. *J. Am. Chem. Soc.* **1992**, *114*, 3978.
(5) Nonell, S.; Arbogast, J. W.; Foote, C. S. *J. Phys. Chem.* **1992**, *96*, 4169.
(6) Ajie, H.; Alvarez, M. M.; Anz, S. J.; Beck, R. D.; Diederich, F.; Fostiropoulos, K.; Huffman, D. R.; Krätschmer, W.; Rubin, Y.; Schriver, K. E.; Sensharma, D.; Whetten, R. L. *J. Phys. Chem.* **1990**, *94*, 8630−8633.
(7) (a) Williams, R. M., Zwier, J. M.; Verhoeven, J. W. *J. Am. Chem. Soc.* **1995**, *117*, 4093 and references cited therein. (b) For a review of the photophysical properties of the fullerenes, see: Foote, C. S. In *Top. Curr. Chem.* **1994**, *169*, 347.
(8) (a) Hirsch, A.; Li, Q.; Wudl, F. *Angew. Chem., Int. Ed. Engl.* **1991**, *30*, 1309. (b) Taylor, R.; Walton, D. R. M. *Nature* **1993**, *363*, 685.
(9) Donor−Acceptor systems containing fullerenes: (a) Maggini, M.; Scorrano, G.; Prato, M. *J. Am. Chem. Soc.* **1994**, *115*, 9798. (b) Kahn, S. I.; Oliver, A. M.; Paddon-Row, M. N.; Rubin, Y. *J. Am. Chem. Soc.* **1993**, *115*, 4919. (c) Belik, P.; Gügel, A.; Kraus, A.; Spickermann, J.; Enkelmann, V.; Frank, G.; Müllen, K. *Adv. Mater.* **1993**, *5*, 854. (d) Maggini, M.; Karlsson, A.; Scorrano, G.; Sandonà, G.; Farnia, G.; Prato, M. *J. Chem. Soc., Chem. Commun.* **1994**, 589. (e) Beer, E.; Feuerer, M.; Knorr, A.; Mirlach, A.; Daub, J. *Angew. Chem., Int. Ed. Engl.* **1994**, *33*, 1087. (f) Iyoda, M.; Sultana, F.; Sasaki, S.; Yoshida, M. *J. Chem. Soc., Chem. Commun.* **1994**, 1929. (g) Diederich, F.; Dietrich-Buchecker, C.; Nierengarten, J.-F.; Sauvage, J.-P.; *J. Chem. Soc., Chem. Commun.* **1995**, 781. (h) Maggini, M.; Donnò, A.; Scorrano, G.; Prato, M. *J. Chem. Soc., Chem. Commun.* **1995**, 845. (i) Linssen, T. G.; Dürr, K.; Hanack, M.; Hirsch, A. *J. Chem. Soc., Chem. Commun.* **1995**, 103.
(10) (a) Liddell, P. A.; Sumida, J. P.; Macpherson, A. N.; Noss, L.; Seely, G. R.; Clark, K. N.; Moore, A. L.; Moore, T. A.; Gust. D. *Photochem. Photobiol.* **1994**, *60*, 537. (b) Imahori, H.; Hagiwara, K.; Akiyama,T.; Taniguchi,S.; Okada, T.; Sakata, Y. *Chem. Lett.* **1995**, 265.

S0022-3263(96)00678-0 CCC: $12.00

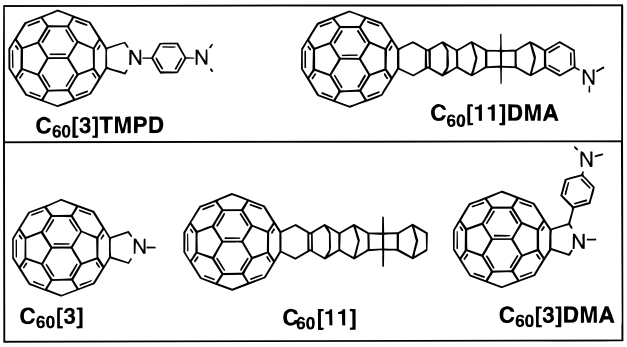

Figure 1. Structures of the dyads **C_{60}[3]TMPD** and **C_{60}[11]-DMA**, the models **C_{60}[3]** and **C_{60}[11]**, and the related dyad **C_{60}[3]DMA** described earlier.

to 11 bonds in **C_{60}[11]DMA**,[11] in an effort to increase the lifetime of the charge-separated state. This "norbornylogous" bridge comprises linearly fused norbornane and bicyclo[2.2.0]hexane units and is well-known to be an efficient mediator of through-bond coupling.[12] We have, in fact, previously demonstrated[13] that separation of an electron donor and acceptor by longer extended hydrocarbon bridges can be applied as a tool to decrease the rate of charge recombination while still maintaining a sufficiently high rate of charge separation.

Experimental Section

Syntheses. The syntheses of the systems **C_{60}[3]DMA**, **C_{60}[3]**,[7a] **C_{60}[11]DMA**, and **C_{60}[11]**[14] have been previously reported. The system **C_{60}[3]TMPD** was synthesized in a similar manner as **C_{60}[3]DMA**, using an *in situ* generation of *N*-(4-(dimethylamino)phenyl)glycine from its ethyl ester, followed by a two-phase water/toluene reaction system for decarboxylation and addition to C_{60} (see supporting information).

Photophysical Measurements. Fluorescence emission and excitation spectra were recorded on a SPEX Fluorolog 2 instrument equipped with a red sensitive GaAs photomultiplier (RCA C31034, Peltier cooled) for which the spectral response extends to ≤900 nm and is known to be quite flat from the UV to about 860 nm.

Fluorescence spectra were measured on dilute solutions (10^{-5} M) using a 570 nm (emission path) cutoff filter. Excitation and emission bandwidths of 4.5 nm were employed, and no corrections were applied to the fluorescence spectra. Long integration times (10 s) and small increments (0.2 nm) were used.

For the determination of the fluorescence quantum yields, C_{60} in non-degassed methylcyclohexane ($\Phi_{fl} = 2 \times 10^{-4}$) was used as a standard.[7a] The excitation wavelength was 470 nm, and the absorbance of both the reference and the sample was adjusted to 0.1 (1 cm) at this wavelength.

Temperature dependent fluorescence measurements were performed with an Oxford Instruments liquid nitrogen DN 1740 cryostat, equipped with an ITC4 control unit. Samples were degassed with three freeze−pump−thaw cycles at *ca.* 10^{-5} mbar. Relative fluorescence intensities were determined by spectral integration.

Table 1. Fluorescence Quantum Yields (Absolute and Relative to Acceptor Reference System C_{60}[3]) of C_{60}[3]TMPD in Various Solvents of Increasing Dielectric Constant (ϵ) and the Rate of Photoinduced Charge Separation (k_{cs}) As Estimated *via* eq 1

solvent	ϵ	Φ_{fl} (relative in %)	k_{cs} (s^{-1})
methylcyclohexane	2.07	1.3×10^{-5} (3)	2.5×10^{10}
toluene	2.38	1.6×10^{-5} (4)	1.9×10^{10}
dichloromethane	8.93	2.0×10^{-5} (4)	1.9×10^{10}
benzonitrile	25.20	3.2×10^{-5} (7)	1.0×10^{10}
dichloromethane/TFA		4.4×10^{-4} (100)	

Absorption spectra were recorded on a CARY 3 spectrophotometer, using a 0.5 nm bandwidth.

Transient absorption (TA) spectra were obtained using a gated optical multichannel analyzer, from EG&G instruments, as described earlier.[15] For excitation and white probe sources, the third harmonic of a Nd-YAG laser (355 nm, nanosecond pulses) and a 450 W high-pressure Xe arc (white light 300−880 nm) coupled to a Müller Elektronik MSP05 pulser were used, respectively. The excitation beam is at right angles to the probing beam. The probing path length is 1 cm. Samples were adjusted to an absorption of 1.5 (1 cm) at the excitation wavelength. Laser power was 7 mJ per pulse (0.2 cm^2). For the determination of the lifetime of the charge-separated state, the sample was degassed with several freeze−pump−thaw cycles.

Fluorescence lifetimes were measured with time-correlated single photon counting using a Hamamatsu microchannel plate (R 3809) detector in a setup slightly modified from that previously described,[16] employing a frequency-doubled DCM dye laser which is synchronously pumped with a mode-locked argon ion laser resulting in 317 nm 20 ps FWHM pulses of 16 nJ. Decays were analyzed with a home-written deconvolution program.

Spectroscopy grade solvents were used in all determinations. Benzonitrile was distilled over P_2O_5 before use.

Semiempirical calculation were performed with a Silicon Graphics Indigo using the package Spartan.[17]

Results and Discussion

Photophysical Properties of Fullerene Adducts. C_{60}[3]TMPD System. The UV−vis absorption of **C_{60}[3]TMPD** is very similar to that reported earlier[7a] for **C_{60}[3]DMA**. However, while the spectral shape of its fluorescence spectrum is also typical for fullerene adducts [see ref 7a, and the next section], the quantum yield is strongly reduced, compared to that of, for example, **C_{60}[3]** in *all* solvents investigated (see Table 1). As we reported earlier,[7a] such a reduction in fluorescence quantum yield occurs for **C_{60}[3]DMA** only in polar solvents. Intramolecular charge separation was implied as the quenching mechanism in the latter system, and this mechanism also appears to be operating in **C_{60}[3]TMPD**, irrespective of solvent polarity. In accordance with this deduction, the quenched local fluorescence of the fullerene chromophore in **C_{60}[3]TMPD** is fully restored upon addition of trifluoroacetic acid (TFA) to a solution of **C_{60}[3]TMPD** in dichloromethane. Protonation of the nitrogen atoms of the TMPD unit reduces its electron-donating capacity and thus prevents charge transfer (see Table 1).

From the relative fluorescence quantum yields in Table 1 and the fluorescence lifetime of **C_{60}[3]** ($\tau_{ref} = 1280$ ps, see ref 7a), an estimate of the charge separation rate

(11) The length of the bridge is taken to be the number of saturated bonds connecting the π-systems of the two chromophores. Thus, one of the saturated bonds of the fullerene cage is also included in the count. In the accompanying paper, only the length of the actual *norbornylogous* bridge was counted.

(12) Paddon-Row, M. N.; Wong, S. S. *Chem. Phys. Lett.* **1990**, *167*, 432

(13) (a) Oevering, H.; Paddon-Row, M. N.; Heppener, M. Oliver, A. M.; Cotsaris, E.; Verhoeven, J. W.; Hush, N. S. *J. Am. Chem. Soc.* **1987**, *109*, 3258. (b) Kroon, J.; Verhoeven, J. W.; Paddon-Row, M. N.; Oliver, A. M. *Angew. Chem., Int. Ed. Engl.* **1991**, *30*, 1358.

(14) Lawson, J. M.; Oliver, A. M.; Rothenfluh, D. F.; An, Y.-Z; Ellis, G. A.; Ranasinghe, M. G.; Khan., S. I.; Franz, A. G.; Ganapathi, P. S.; Shephard, M. J.; Paddon-Row, M. N.; Rubin, Y. *J. Org. Chem.* **1996**, *61*, 5032.

(15) Van Stokkum, I. H. M.; Scherer, T.; Brouwer. A. M.; Verhoeven, J. W. *J. Phys. Chem.* **1994**, *98*, 852.

(16) Bebelaar, D. *Rev. Sci. Instrum.* **1986**, *57*, 1116.

(17) SPARTAN version 4.0.1; Wavefunction Inc.; 18401 Von Karman Ave, Suite 370, Irvine, CA 92715.

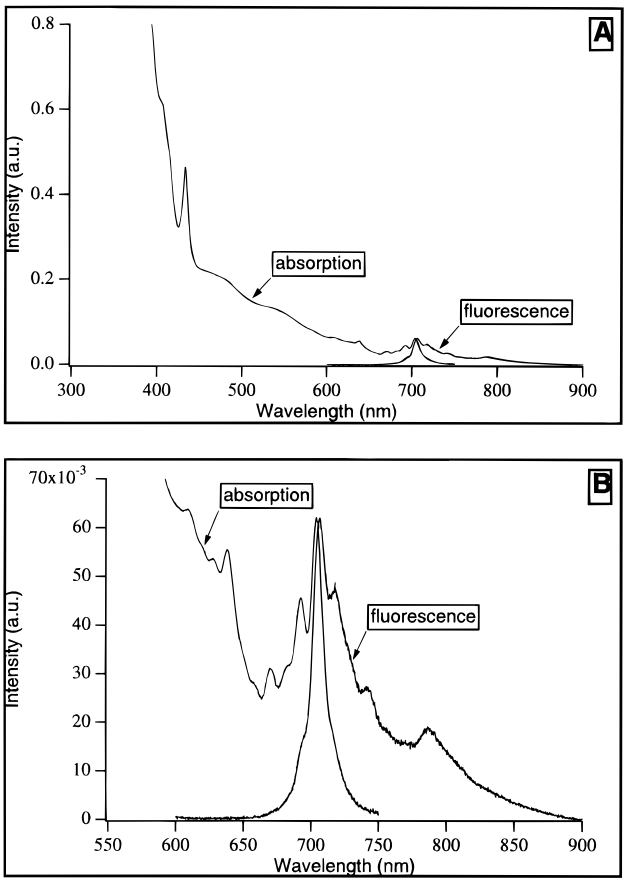

Figure 2. Vis absorption and fluorescence emission spectra of compound **C_{60}[11]DMA** in methylcyclohexane at room temperature (A, full range; B, expansion above 550 nm).

constant (k_{cs}) can be made *via* eq 1:

$$k_{cs} = (\Phi_{ref}/\Phi - 1)/\tau_{ref} \quad (1)$$

The results of this estimate are compiled in the last column of Table 1.

Interestingly, in contrast to **C_{60}[3]DMA**, the rate of photoinduced charge separation in **C_{60}[3]TMPD** displays only a minor solvent dependence (if any) even tends to decrease in more polar solvents. As we have discussed previously,[13b] this implies that charge separation occurs under nearly optimal conditions in the sense of the Marcus theory. Under such conditions, the effect of increasing the driving force by moving to more polar solvents can be fully compensated, or even slightly overcompensated, by the concomitant increase in solvent reorganization energy.

While an increase in the donor strength at constant bridge length resulted in optimization of the charge separation process, nanosecond time scale TA measurements performed on **C_{60}[3]TMPD** in various solvents did not allow any transient to be observed. Thus in all solvents the lifetime of the charge-separated state is below the nanosecond time scale, as observed earlier for the **C_{60}[3]DMA** system,[7a] as well as for other donor−bridge−C_{60} systems involving a short bridge[10] in polar solvents.

The C_{60}[11]DMA and C_{60}[11] Systems. The absorption and fluorescence spectra and the T_1-T_n absorption spectrum of **C_{60}[11]DMA** in nonpolar media are very similar to those reported earlier for the analogous system **C_{60}[3]DMA**.[7a] Figure 2 shows the fluorescence and the vis absorption spectra of **C_{60}[11]DMA** in methylcyclohexane.

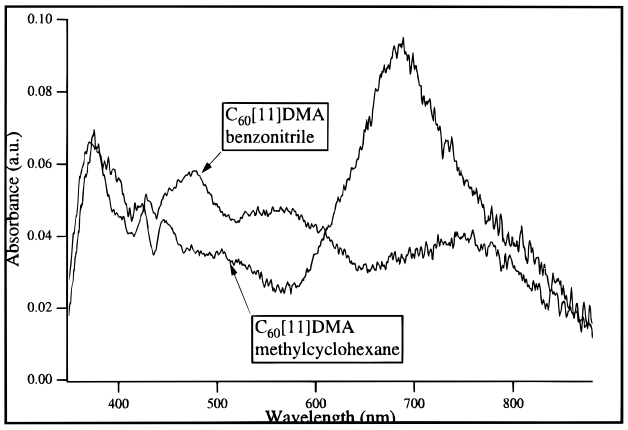

Figure 3. Transient absorption spectra of **C_{60}[11]DMA** in methylcyclohexane and in benzonitrile.

Table 2. Fluorescence Quantum Yields (Absolute and Relative) of C_{60}[11]DMA in Solvents with Various Dielectric Constants

solvent	ϵ	Φ_{fl} (relative in %)
methylcyclohexane	2.07	4.37×10^{-4} (100)
toluene	2.38	4.26×10^{-4} (97)
1,4-dioxane	2.21	2.32×10^{-4} (53)
1,2-dichlorobenzene	9.93	1.35×10^{-4} (30)
benzonitrile	25.20	0.56×10^{-4} (12)

Absorption maxima are observed at 406 (sh), 434, 480 (sh), 548 (sh), 609, 614, 638, 670, 682 (sh), 692, 703.8, and 717 nm (which is presumably a hot band). Fluorescence maxima are observed at 690 (hot band), 706.6, 718, 742, and 787 nm. The system has a very minor Stokes shift (56 cm^{-1}) and an $^1E_{00}$ of 1.76 eV (705 nm).

The fluorescence excitation spectra for **C_{60}[11]DMA** are in excellent agreement with its absorption spectra, indicating "normal" photophysical behavior and the absence of interfering impurities.

Fluorescence quantum yields of **C_{60}[11]DMA** in different solvents are given in Table 2. Interestingly, and in analogy to **C_{60}[3]DMA**, the fluorescence intensity decreases markedly on going to more polar solvents (see Table 2).

By contrast, **C_{60}[11]** displays a virtually solvent independent fluorescence (quantum yield = 4.05×10^{-4}), analogous to the behavior of **C_{60}[3]**. Both the fluorescence of **C_{60}[11]DMA** and its TA spectrum show a marked solvent dependence. Thus, in nonpolar solvents the nanosecond TA spectra of **C_{60}[11]DMA** and **C_{60}[11]** are identical and are very similar to that described earlier[7a] for **C_{60}[3]**. These spectra stem from the triplet state of the fullerene unit which is populated *via* the fast and almost quantitative intersystem crossing in the C_{60} chromophore. While **C_{60}[11]** and **C_{60}[3]** still display the same TA spectra in polar media, the TA spectrum of **C_{60}[11]DMA** changes drastically. Thus, in benzonitrile (see Figure 3) a characteristic absorption around 460 nm is observed, and this is attributed to the radical cation of the dimethylaniline chromophore, with a lifetime of 0.25 μs!

Furthermore, absorptions at 750 and especially at 590 nm, which can be attributed to the radical anion of the fullerene moiety,[9e] possess the same lifetime as the radical cation of the dimethylaniline chromophore.

The ratio of signal intensities for the **C_{60}[11]DMA** samples in methylcyclohexane and benzonitrile (taken

Table 3. Primary Data Used for the Determination of the Barrier to Charge Separation for C_{60}[11]DMA in Benzonitrile Relative Emission Yield (Φ_{rel}) at Temperature (T) Together with the Rate of Electron Transfer Obtained *via* eq 1

T (K)	Φ_{rel}	k_{cs} (s^{-1})
295	1	4.74×10^9
290	1.05	4.47×10^9
285	1.09	4.27×10^9
280	1.14	4.04×10^9
275	1.20	3.82×10^9
270	1.26	3.59×10^9
265	1.34	3.33×10^9

under similar conditions) is almost equal to the ratio of the extinction coefficients of, respectively, the triplet−triplet absorption of the fullerene moiety (16700 L mol^{-1} cm^{-1} at 692 nm)[7a] and the dimethylaniline radical cation (4800 L $mol^{-1}cm^{-1}$ at 460 nm).[18] This indicates that the yield of charge transfer state formation in benzonitrile is ≥90%.

The solvent dependence of the fluorescence and the TA spectra for **C_{60}[11]DMA** clearly indicate that in polar solvents an intramolecular charge separation occurs that quenches the locally excited state, thereby creating a long-lived charge transfer state.

While earlier preliminary time-resolved fluorescence experiments[19] on **C_{60}[11]DMA**, in which the DMA chromophore was excited, indicated that the UV emission emerging from this chromophore is strongly quenched by energy (or electron) transfer, the fluorescence decays now observed for the red emission at 707 nm of the fullerene using single photon counting in methylcyclohexane give a fluorescence lifetime of 1344 ± 10 ps for both **C_{60}[11]-DMA** and **C_{60}[11]**. In the polar solvent benzonitrile, in which both luminescence and population of the triplet state for **C_{60}[11]DMA** are strongly quenched, fluorescence decay from the fullerene unit displays a major fast component of 160 ± 10 ps.

The rate of charge separation for **C_{60}[11]DMA** in benzonitrile is estimated from eq 2 to be $k_{cs} = 5.5 \times 10^9$ s^{-1}:

$$k_{cs} = 1/\tau - 1/\tau_{ref} \qquad (2)$$

In this equation, the lifetime of **C_{60}[11]DMA** (or **C_{60}[11]**) in methylcyclohexane is taken to be equal to τ_{ref}. Application of eq 1 to the quantum yield data from Table 2 gives a quite similar value for k_{cs}: 5.1×10^9 s^{-1}.

From these data the quantum yield for charge separation *via* the excited singlet state of the fullerene unit is estimated to be $k_{cs}/[1/\tau_{ref} + k_{cs}] \times 100 = 87-88\%$, which is in excellent agreement with the estimate made from the transient absorption spectra.

In order to determine the barrier for electron transfer experimentally, the temperature dependence of the fluorescence quantum yield of **C_{60}[11]DMA** in benzonitrile was investigated (see Table 3 for primary data). As a reference, **C_{60}[11]** was employed, for which the fluorescence quantum yield is virtually temperature independent. From these measurements, electron transfer rates were derived *via* eq 1. Linear regression for a plot (see Figure 4) of the natural logarithm of the electron transfer rates multiplied by the square root of T, as a function of

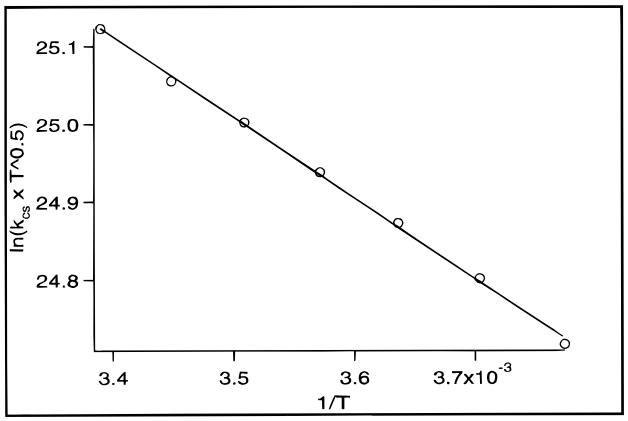

Figure 4. Modified Arrhenius plot $\ln(k_{cs} \times \sqrt{T}) = \ln(k_{opt}) - (\Delta G^{\#}_{cs}/k_B) \times 1/T$ for **C_{60}[11]DMA** obtained in benzonitrile.

$1/T$, leads to an intercept of 28.64 (= ln k_{opt} (s^{-1} $K^{0.5}$)) and a slope of 1038.1 (= $\Delta G^{\#}/k_B$ (K)). The barrier of electron transfer is therefore determined[20] to be $\Delta G^{\#} =$ 0.09 eV, and the charge separation rate under barrierless conditions (k_{opt}) is $2.75 \times 10^{12} \times T^{1/2}$ (s^{-1} $K^{0.5}$).

The conformation of the adduct **C_{60}[11]DMA** obtained by energy minimization[21] with semiempirical AM1 calculations is shown in Figure 5. The center-to-center distance between the two chromophores is estimated to be *ca.* 18 Å; the edge-to-edge distance is *ca.* 12.6 Å.

With these geometrical data in hand, together with the electrochemical and photophysical data for the constituent chromophores, the barrier to photoinduced electron transfer can also be predicted, in principle, from the Marcus equation (3):

$$\Delta G^{\#}_{cs} = (\Delta G_{cs} + \lambda)^2/4\lambda \qquad (3)$$

Here, ΔG_{cs} is the Gibbs free energy change and λ the total reorganization energy. The former can be approximated as proposed by Weller *et al.*[22] *via*

$$\Delta G_{cs} = e(E^{ox}(D) - E^{red}(A)) - E_{00} - e^2/4\pi\epsilon_o\epsilon_s R_c - e^2/8\pi\epsilon_o(1/r^+ + 1/r^-)(1/37.5 - 1/\epsilon_s) \qquad (4)$$

Calculation of ΔG_{cs} from eq 4 requires, in addition to the donor and acceptor redox potentials (+0.71 V and −0.57 V *vs* SCE) and the singlet or triplet state energy ($^1E_{00} = 1.76$ eV and $^3E_{00} = 1.50$ eV), [7a] knowledge of the center-to-center distance (R_c) and the effective ionic radii of the donor and acceptor radical cation and anion (r^+ and r^-, respectively). A value of 18 Å was estimated for R_c from our modeling results (Figure 5). Values for r^+ and r^- were calculated from the apparent molar volumes of *N*,*N*-dimethylaniline (density = $\rho = 0.956$) and of C_{60} (density 1.65), using a spherical approach.

$$^4/_3\pi r^3 = M/n\rho \qquad (5)$$

Here, M is the molecular weight and N is Avogadro's number. This gives $r^+ = 3.7$ Å and $r^- = 5.6$ Å. The

(18) Shida, T. *Electronic absorption spectra of radical ions* (physical science data; 34) Elsevier Science Publishers: Amsterdam, 1988.

(19) In *n*-hexane an energy or electron transfer rate of ca. 1.2×10^{10} s^{-1} was observed; private communication from A. H. A. Clayton and K. P. Ghiggino, 1995.

(20) (a) Kroon J.; Oevering, H.: Verhoeven, J. W.; Warman, J. M.; Oliver, A. M.; Paddon-Row, M. N. *J. Phys. Chem.* **1993**, *97*, 50675. (b) Zeng, Y.; Zimmt, B.; *J. Phys. Chem.* **1992**, *96*, 8395.

(21) The conformation shown in Figure 5 is the lowest energy conformation; however another conformation is possible, which is slightly higher in energy, see accompanying paper in this issue.

(22) Weller, A. *Z. Phys. Chem., Neue Folge* **1982**, *133*, 93.

Table 4. Reorganization Energy ($\lambda = \lambda_s + 0.3$ eV), Gibbs Free Energy Change (ΔG_{cs}), and Barrier ($\Delta G^{\#}_{cs}$) for Charge Separation in Various Solvents (Dielectric Constant ϵ, Refractive Index n) from Both the Singlet and Triplet (T) State of the Fullerene Chromophore in C60[11]DMA, As Calculated *via* eqs 3, 4, and 6

				charge separation			
				from singlet state		from triplet state	
solvent	ϵ	n	λ (eV)	ΔG_{cs} (eV)	$\Delta G^{\#}_{cs}$ (eV)	ΔG_{cs}(T) (eV)	$\Delta G^{\#}_{cs}$(T) (eV)
methylcyclohexane	2.07	1.423	0.33	0.61	0.58	0.87	1.09
1,4-dioxane	2.209	1.422	0.36	0.53	0.40	0.79	0.80
toluene	2.38	1.497	0.40	0.50	0.48	0.72	0.35
diethyl ether	4.20	1.35	1.01	0.01	0.25	0.27	0.28
1,2-dichlorobenzene	9.93	1.552	1.02	−0.32	0.12	−0.06	0.23
benzonitrile	25.20	1.528	1.20	−0.47	0.11	−0.21	0.20

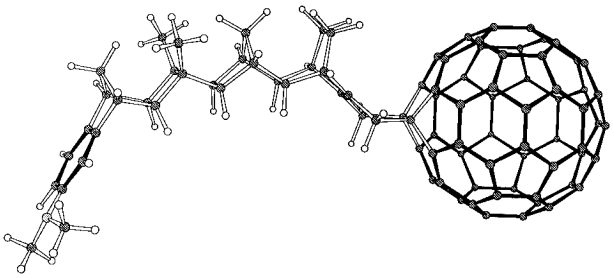

Figure 5. Structure of **C_{60}[11]DMA** obtained with AM1.

calculated ΔG_{cs} values in various solvents are listed in Table 4 for both singlet and triplet charge separation.

The reorganization energy λ may be partitioned into internal (λ_i) and solvent (λ_s) contributions. The internal reorganization energy was set at $\lambda_i = 0.3$ eV,[7a] while λ_s was calculated[13] using the Born−Hush approach (eq 6):

$$\lambda_s = e^2/4\pi\epsilon_o(1/r - 1/R_c)(1/n^2 - 1/\epsilon_s) \qquad (6)$$

In agreement with the fluorescence data discussed above, it is found that the driving force for charge separation ($-\Delta G_{cs}$) from the fullerene S_1 state becomes positive in solvents more polar than diethyl ether.[23] Furthermore, the calculated barrier (0.11 eV) for electron transfer in benzonitrile is in reasonable agreement with the experimental value (0.09 eV). As we have shown earlier,[20a] this agreement and the high linearity of the Arrhenius plot obtained (see Figure 4) are typical for electron transfer processes taking place in the "normal" Marcus region if performed in polar media.

It is important to note that, due to the relatively small S_1-T_1 energy gap of the fullerene chromophore, photoinduced charge separation from the T_1 state can also become exergonic in sufficiently polar media such as benzonitrile (see Table 4). As discussed above, however, charge separation from the S_1 state is so rapid in this solvent that it accounts for *ca.* 90% of the fullerene's S_1 decay modes, thereby overwhelming the otherwise efficient intersystem crossing of the fullerene chromophore ($k_{isc} \approx 7.5 \times 10^8$ s^{-1}).

Evaluation of the Electronic Coupling Matrix Element for Charge Separation in C_{60}[11]DMA. The high rates of charge separation and recombination in **C_{60}[3]DMA** and **C_{60}[3]TMPD** are not surprising in view of the fact that bridges with an effective length of three σ bonds are known to provide quite strong through-bond and though-space electronic coupling between the D and A units, which may even be sufficiently strong to bring the electron transfer processes into the adiabatic regime.

The high rate of photoinduced charge separation, as opposed to the relatively slow recombination in **C_{60}[11]DMA**, is surprising because both the calculated and experimentally determined barriers to charge separation (0.11 and 0.09 eV, respectively) are significantly higher than in systems for which we have previously observed fast photoinduced charge separation across bridges of similar length.[13] It is therefore interesting to compare the electronic coupling matrix element (V^*) involved in the excited state charge separation process for **C_{60}[11]DMA** with that determined earlier for other bridged systems. This can be done readily using the nonadiabatic expression for electron transfer processes[20a] given by eq 7:

$$k_{cs} = \frac{2\pi^{3/2}}{h\sqrt{\lambda k_B T}}(V^*)^2 \exp\left[\frac{-\Delta G^{\#}_{cs}}{k_B T}\right] \qquad (7)$$

Substitution of k_{cs}(5.5 × 10^9 s^{-1} at 300 K) and $\Delta G^{\#}_{cs}$ (0.09 eV), together with an estimated total reorganization energy of 1.2 eV (see Table 4), leads to $V^* = 28$ cm^{-1}. Table 5 presents a compilation of values of coupling matrix elements for excited state electron transfer (V^*) and for thermal electron transfer (V) in a variety of donor−bridge−acceptor systems possessing effective bridge lengths ranging from four to ten σ bonds. In Figure 6, the V and V^* values are plotted semilogarithmically against the number, n, of σ bonds in the bridge for each series of systems. The plots display the expected (approximate) exponential decay of V and V^* with bridge length (n).

In spite the fact that the data compiled in Table 5 refer to a variety of bridges and D/A chromophores, it is evident that the V^* value of *ca.* 30 cm^{-1} derived for **C_{60}[11]DMA** is exceptionally large, and in fact exceeds the expected value for an 11-bond bridge by about an order of magnitude. The only report of similarly large V values refers to extrapolation of the work of Penfield *et al.*,[28] who measured the intervalence absorption bands in the anion radicals of the **DMN[*n*]DCV** series of molecules, arising from through-bond electronic coupling between the 1,1-dicyanovinyl (DCV) radical anion and the 1,4-dimethoxynaphthalene (DMN) unit, across 4-, 6-, and 8-bond

(23) It should be noted that the occurrence of charge separation in 1,4-dioxane once more testifies the high micropolarity of this quadrupolar solvent, see: Suppan, P. *J. Photochem. Photobiol. A* **1990**, *50*, 293.

(24) It should be noted that this is a lower limit since substitution of the rate (5.5 × 10^9 s^{-1}) and the barrier (0.11 eV) calculated *via* the Marcus equation (see Table 3) gives a value as high as 44 cm^{-1}.

(25) Closs, G. L.; Miller, J. R. *Science* **1988**, *240*, 440.

(26) Oevering, H.; Verhoeven, J. W.; Paddon-Row, M. N.; Warman, J. M. *Tetrahedron* **1989**, *45*, 4751.

(27) Stein, C. A.; Lewis, N. A.; Seitz, G. *J. Am. Chem. Soc.* **1982**, *104*, 2596.

(28) Penfield, K. W.; Miller, J. R.; Paddon-Row, M. N.; Cotsaris, E.; Oliver, A. M.; Hush, N. S. *J. Am. Chem. Soc.* **1987**, *109*, 5061.

Table 5. Experimental Values for the Electronic Coupling Matrix Element $V^{(*)}$ for Excited State (V) or Thermal (V^*) Electron Transfer Processes between Electron Donor and Acceptor Sites Connected by Extended Arrays of n σ Bonds

Structure	n	$V^{(*)}$ (cm^{-1})
Np–BP$^{-\cdot}$	5	128[a]
Np–BP$^{-\cdot}$	6	54[a]
Np–BP$^{-\cdot}$	7	30[a]
Np–BP$^{-\cdot}$	10	6.2[a]
MeO, CN, CN, MeO — DMN[4]DCV	4	370[b]
MeO, CN, CN, MeO — DMN[6]DCV	6	112[b]
MeO, CN, CN, MeO — DMN[8]DCV	8	40[b]
MeO, CN, CN, MeO — DMN[10]DCV	10	17.6[b]
$(H_3N)_5Ru^{II}$–S–S–$Ru^{III}(NH_3)_5$	4	138[c]
$(H_3N)_5Ru^{II}$–S–S–$Ru^{III}(NH_3)_5$	6	55[c]
$(H_3N)_5Ru^{II}$–S–S–$Ru^{III}(NH_3)_5$	8	24[c]

[a] From the rate of electron transfer of an anion radical centered on the BP (biphenyl) to the naphthalene (Np) unit.[25] [b] From the radiative rate constant of charge transfer fluorescence.[26] [c] From the inter valence absorption.[27]

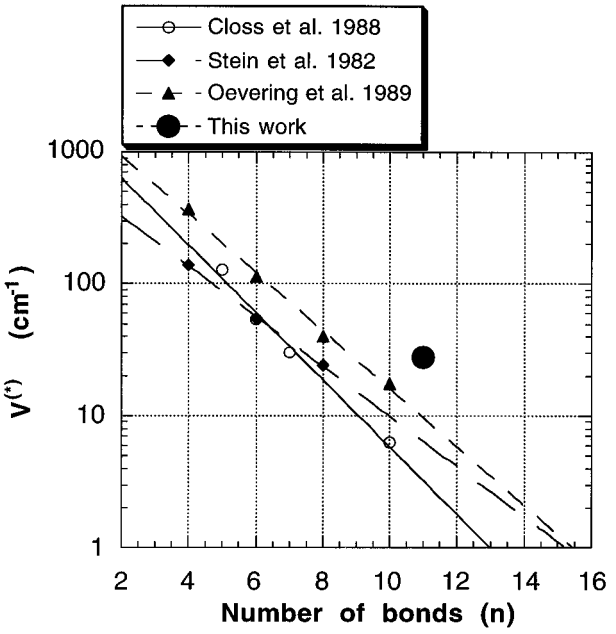

Figure 6. Semilogarithmic plot of various data sets from Table 5, showing the approximate exponential decay of $V^{(*)}$ with bridge length (n) and the extraordinary large value of V^* for the **C_{60}[11]DMA** system.

bridges. However, measurements of V^* for photoinduced charge separation in the neutral **DMN[*n*]DCV** compounds by Oevering *et al.*[13] gave much smaller values, which are much more in line with results obtained for other systems (see Table 5 and Figure 6). In the context of the Penfield *et al.* experiment, it should be noted that the radical anion of the DCV group is prone to distort by twisting about the C=C double bond, thereby concentrating the unpaired electron on the carbon atom of the vinyl

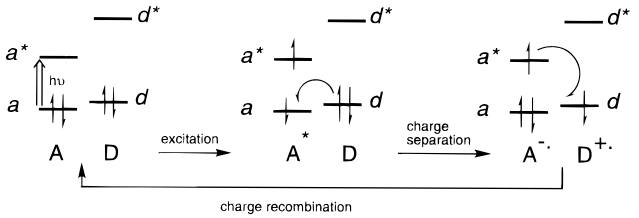

Figure 7. FMO representation of charge separation and charge recombination following local excitation of the acceptor in a D/A system.

group that is attached to the bridge. This may well enhance the magnitude of the electronic coupling, V, in the anion radicals of these systems and it is, therefore, even more striking that with the very diffuse C_{60} acceptor an even stronger coupling in **C_{60}[11]DMA** is achieved.

We tentatively propose that the large V^* for **C_{60}[11]-DMA** is mainly related to the special orbital symmetry properties of the fullerene π–system. Preliminary semiempirical MO calculations are presented in the next section which lend support to this view.

Molecular Orbital Calculations. A simple frontier molecular orbital (FMO) description of photoinduced electron transfer in a D/A system in which the acceptor has the lowest excited state is given in Figure 7.

The HOMOs and LUMOs of D and A are labelled d, d* and a, a*, respectively. Local acceptor excitation (a → a*) is followed by electron transfer involving orbital interactions between d and a, while charge recombination involves interactions between a* and d. The FMO description is undoubtedly an oversimplification, which may, for example, neglect important interactions between charge transfer configurations and locally excited configurations.[29] Nevertheless, it is a useful starting point for identifying important orbital interactions that contribute to the electronic coupling matrix elements involved in the photoinduced charge separation step, following local acceptor excitation (i.e., V^* is related to d/a interaction), and in the subsequent thermal charge recombination step (i.e., V is related to a*/d interaction).

The MOs a, a* and d of **C_{60}[11]DMA** are shown in Figures 8–10. These were obtained from AM1 calculations. Although the frontier orbitals are mainly localized on D or on A, it turns out that the highest occupied orbital of A (i.e., a) is extensively delocalized into the bridge and tailing out all the way into the donor domain (see Figure 8). Importantly, such delocalization into the bridge is found to a much lesser extent for a* (see Figure 9) and for d (see Figure 10).

Although the AM1 calculations were performed on the ground state molecule and the electron densities in certain areas will certainly change if UHF calculations on the excited states and anionic or cationic species are performed, we presume that the extensively delocalized character of a is a consequence of the special symmetry properties of the fullerene π–system. The relevant (pseudo) symmetry planes of the C_{60} π-system are shown in Figure 11.

For planar π-systems such as that of naphthalene, plane **II** coincides with the nodal plane to which all π orbitals are antisymmetric. While this is a typical property of any "normal" π-system, the a orbital of the fullerene system behaves quite atypical in being sym-

(29) Bixon, M.; Jortner, J. Verhoeven, J. W.; *J. Am. Chem. Soc.* **1994**, *116*, 7349.

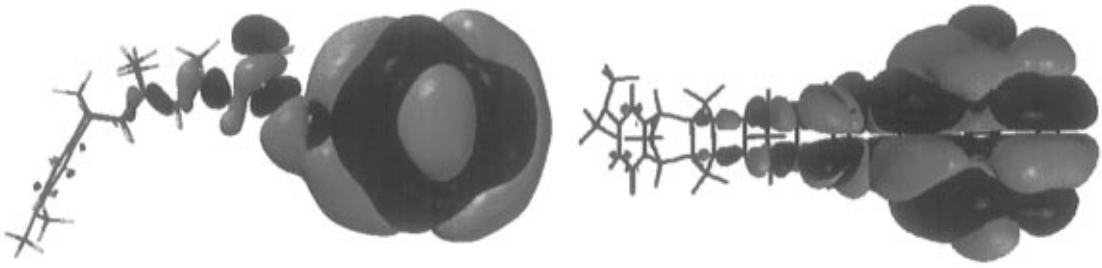

Figure 8. Visualization of orbital a of the donor−bridge−fullerene(acceptor) system in "side" (left) and "top" (right) view, obtained from AM1 calculations, using a value of 0.001 electron/au^3.

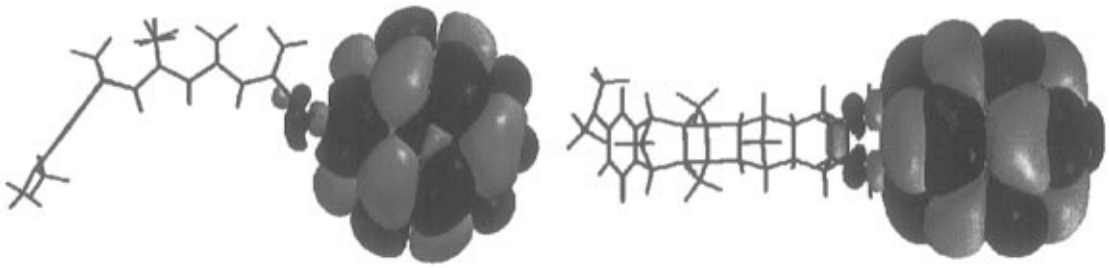

Figure 9. Visualization of orbital a* of the donor−bridge−fullerene(acceptor) system in "side" (left) and "top" (right) view, obtained from AM1 calculations, using a value of 0.001 electron/au^3.

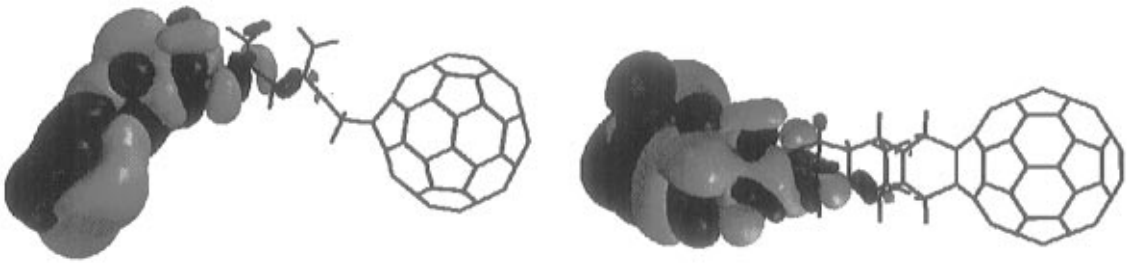

Figure 10. Visualization of d of the donor−bridge−fullerene(acceptor) system in "side" (left) and "top" (right) view, obtained from AM1 calculations, using a value of 0.001 electron/au^3.

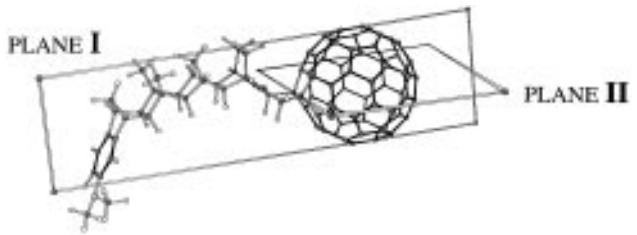

Figure 11. Representation of the (pseudo)symmetry planes of the fullerene π-system in **C_{60}[11]DMA**.

metrical with respect to plane **II**. As schematized in Figure 12 this allows orbital a of the fullerene to interact with the first carbon−carbon bond σ orbitals of the attached bridge (*geminal* bonds). By contrast, normal π orbitals, such as those of naphthalene, cannot couple with the geminal carbon−carbon orbitals of the bridge but only with the next bonds of the bridge (i.e., the *vicinal* bonds).

The fullerene−bridge coupling occurs through *12* $\pi-\sigma$ interactions, as opposed to only two $\pi-\sigma$ interactions for the case of planar π-chromophores. As indicated in the lower part of Figure 12, there are a total of eight vicinal (v) interactions and four geminal (g) interactions. The latter are strongly influenced by the pyramidal character of the C_{60} carbon atoms. Together, these couplings might well amount to a sizeable overall coupling matrix element.

This expectation is borne out by a preliminary natural bond orbital analysis[30] which found that the strengths of the individual v and g couplings in the fullerene−bridge system are 1.0 and 0.7 eV, respectively, and are only slightly smaller than the value of 1.1 eV for each of the v pathways in the naphthalene−bridge system.[31]

It seems important to note that whereas the fullerene HOMO a has the correct symmetry to mix with the bridge σ-HOMO, it cannot interact with the (symmetric) π orbital of the proximate double bond of the cyclohexene ring. Thus no contribution of the latter is found in a (see Figure 8) and the role of this double bond in mediating electron transfer appears to be minor, if any.

While the combination of pyramidalization of the constituent carbon atoms of the fullerene moiety, together with the matching (pseudo)symmetry properties of the fullerene HOMO a and the bridge σ-HOMO, might explain the exceptionally large electronic coupling (V*) for photoinduced charge separation for **C_{60}[11]DMA**, it should be noted that the orbitals involved in the charge recombination process, a* and d (Figure 7), do not delocalize as strongly into the bridge. Orbital d does

(30) (a) Reed, A. E.; Curtiss, L. A.; Weinhold, F. *Chem. Rev.* **1988**, *88*, 899. (b) Jordan, K. D.; Paddon-Row, M. N. *Chem. Rev.* **1992**, *92*, 395. (c) Naleway, C. A.; Curtiss, L. A.; Miller, J. R. *J. Phys. Chem.* **1991**, *95*, 8434. (d) Liang, C.; Newton, M. D. *J. Phys. Chem.* **1992**, *96*, 2855.

(31) Shephard M. J.; Paddon-Row M. N., to be published.

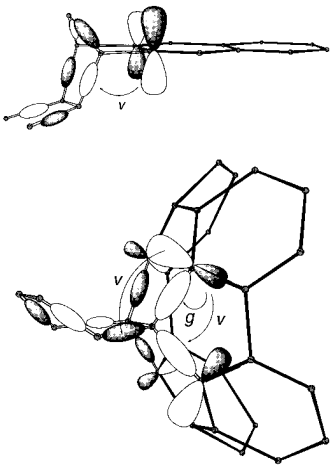

Figure 12. Schematic representation of the coupling of the HOMO of a normal aromatic π-system such as naphthalene (top) and the HOMO (a) of the fullerene π-system (bottom) with the σ bonds of the attached bridge. Note that, because of symmetry restrictions, coupling with the geminal σ bonds of the bridge is not possible for the normal π-system (top). For certain fullerene orbitals (e.g., the HOMO a, see Figure 8) coupling with the geminal σ bonds is possible on account of the special symmetry properties of the fullerene π-system. Both the geminal (g) and the vicinal (v) interactions are indicated.

extend into the bridge, in a very skewed way, but it does not extend all the way to the fullerene acceptor. Although the fullerene LUMO a* is (pseudo)symmetric with respect to plane **II**, it is also symmetric with respect to plane **I**. The latter symmetry property enables it to mix with the bridge σ*-LUMO (which is symmetric with respect to plane **I**), but not with the bridge σ-HOMO (which is antisymmetric, Figure 12). Since it is known[32] that π* orbitals couple strongly with the bridge σ orbitals, as well as with the bridge σ* orbitals, through-bond coupling involving the fullerene MO a* might be weaker than that involving the MO a. Consequently, charge recombination is not expected to be unusually fast, and indeed, the long lifetime of the charge-separated state (0.25 μs) appears to substantiate this, making the **C_{60}[11]DMA** dyad act in a "photodiode" fashion.

Concluding Remarks

The results presented above clearly indicate that excitation of **C_{60}[11]DMA** in a polar solvent (benzonitrile) gives rise to rapid charge separation, resulting in the formation of a long-lived charge-separated state. The ratio between the rates of charge separation and charge recombination for this system in is in fact more than 3 orders of magnitude ($k_{cs}/k_{cr} = 1400$), where the estimated energy gap between the charge-separated state and the ground state ($\Delta G_{cr} \approx -1.29$ eV) in benzonitrile solvent is comparable to the total reorganization energy ($\lambda \approx 1.2$ eV). Thus charge recombination cannot be slowed down significantly by "inverted region effects" as clearly is in systems such as those studied by Oevering *et al.* (see Table 5) in nonpolar media.

The exceptional photodiode properties of the **C_{60}[11]DMA** dyad thus seem to be mostly due to the a high ratio of the electronic coupling elements for charge separation and charge recombination (V^*/V), which is attributed to a combination of the symmetry properties of the fullerene π-system and the pyramidal nature of the fullerene constituent carbon atoms. This may provide a new approach to the design of donor−bridge−acceptor systems with enhanced k_{cs}/k_{cr} ratios, irrespective of solvent polarity. This goal may be achieved, in part, by replacing the *N*,*N*-dimethylaniline donor group in **C_{60}[11]DMA** with a more powerful donor moiety, such that the charge separation step takes place under essentially barrierless conditions. In view of the results presented for the **C_{60}[3]TMPD** system, which contains the strong *p*-phenylenediamine donor, it is likely that systems utilizing the equally potent *o*-phenylenediamine donor group might lead to systems that display fast and virtually barrierless charge separation, while at the same time maintaining a long lifetime of the charge-separated state, irrespective of solvent polarity. Such covalently functionalized donor−bridge−fullerene (acceptor) systems could then turn out to be interesting molecular building blocks in optoelectronic devices.

Acknowledgment. We thank A. H. A. Clayton and K. P. Ghiggino for making available the results of their measurements [ref 19] on quenching of the DMA singlet state in **C_{60}[11]DMA**. The present research was supported by the Netherlands Foundation for Chemical Research (SON) with financial aid from the Netherlands Organization for the Advancement of Scientific Research (NWO) and the Australian Research Council.

Supporting Information Available: Details of the synthesis and identification of **C_{60}[3]TMPD** including spectral data (3 pages). This material is contained in libraries on microfiche, immediately follows this article in the microfilm version of the journal, and can be ordered from the ACS; see any current masthead page for ordering information.

JO960678Q

(32) Balaji, V.; Ng, L.; Jordan, K. D.; Paddon-Row, M. N.; Patney, H. K. *J. Am. Chem. Soc.* **1987**, *109*, 6957.